



HAL
open science

Increasing entanglement between Gaussian states by coherent photon subtraction

Alexei Ourjoumtsev, Aurelien Dantan, Rosa Tualle-Brouri, Philippe Grangier

► **To cite this version:**

Alexei Ourjoumtsev, Aurelien Dantan, Rosa Tualle-Brouri, Philippe Grangier. Increasing entanglement between Gaussian states by coherent photon subtraction. *Physical Review Letters*, 2007, 98, pp.030502. 10.1103/PhysRevLett.98.030502. hal-00090186v4

HAL Id: hal-00090186

<https://hal.science/hal-00090186v4>

Submitted on 29 Jan 2007

HAL is a multi-disciplinary open access archive for the deposit and dissemination of scientific research documents, whether they are published or not. The documents may come from teaching and research institutions in France or abroad, or from public or private research centers.

L'archive ouverte pluridisciplinaire **HAL**, est destinée au dépôt et à la diffusion de documents scientifiques de niveau recherche, publiés ou non, émanant des établissements d'enseignement et de recherche français ou étrangers, des laboratoires publics ou privés.

Increasing entanglement between Gaussian states by coherent photon subtraction

Alexei Ourjoumtsev, Aurélien Dantan, Rosa Tualle-Brouri, and Philippe Grangier
*Laboratoire Charles Fabry de l'Institut d'Optique, CNRS UMR 8501, 91403 Orsay, France**

(Dated: January 30, 2007)

We experimentally demonstrate that the entanglement between Gaussian entangled states can be increased by non-Gaussian operations. Coherent subtraction of single photons from Gaussian quadrature-entangled light pulses, created by a nondegenerate parametric amplifier, produces delocalized states with negative Wigner functions and complex structures more entangled than the initial states in terms of negativity. The experimental results are in very good agreement with the theoretical predictions.

PACS numbers: : 03.67.-a, 03.65.Wj, 42.50.Dv

Entanglement plays a key role in quantum information processing (QIP). Entanglement distillation [1], demonstrated for discrete-variable systems (ebits) in recent experiments [2, 3, 4], allows one to produce strong entanglement between distant sites, initially sharing a larger set of weakly entangled states, and constitutes the basis of quantum repeaters, essential for long-distance quantum communications. An interesting alternative to discrete-level systems are quantum continuous variables (QCVs). In this case the information is encoded in the quadratures \hat{x} and \hat{p} of traveling light fields, which can be efficiently measured by homodyne detection. Optical parametric amplification allows one to produce quadrature-entangled beams, used in many QIP protocols. Together with linear optics, these tools preserve the Gaussian character of the states involved in most of QCV experiments: the quasi-distributions (Wigner functions) of their quadratures remain Gaussian. However, it has been shown that Gaussian entanglement distillation requires non-Gaussian operations [5, 6, 7]. Among several proposals [8, 9], one of the simplest is the conditional subtraction of photons from Gaussian entangled beams [10, 11, 12, 13], by reflecting a small part of these beams towards two photon-counting avalanche photodiodes (APDs). If the reflectivity is low, a simultaneous detection of photons by the APDs heralds the subtraction of exactly one photon from each beam. Recently, such methods allowed the preparation and analysis of several states with negative Wigner functions, including one- and two-photon Fock states [14, 15, 16], delocalized single photons [17, 18] and photon-subtracted squeezed states, very similar to quantum superpositions of coherent states with small amplitudes [19, 20].

In this Letter, we experimentally demonstrate that non-Gaussian operations allow us to increase the entanglement between Gaussian states, with a protocol presented on Fig. 1. An optical parametric amplifier (OPA) produces Gaussian quadrature-entangled light pulses, known as two-mode squeezed states [21]. We pick off small fractions of these beams, which interfere with a well-defined phase on a 50/50 beam splitter (BS), and we detect photons in one of the BS outputs. This way,

we subtract a *single* photon delocalized in the two beams and prepare a complex quantum state with a negative two-mode Wigner function. We determine a range of experimental parameters where the entanglement of the prepared state, quantified by the negativity [22], is significantly higher compared to that of the initial Gaussian state.

Operating with single photon counts rather than with coincidences as proposed e. g. in [10, 11, 12, 13, 23, 24], this protocol allows for much higher generation rates and produces states more robust to experimental imperfections (see below). Besides, it is more efficient at moderate OPA gain: in the zero-gain limit, the detection of a photon transforms a state with almost no entanglement into a maximally entangled ebit state $(|10\rangle + |01\rangle)/\sqrt{2}$. With the higher gain (up to 3 dB) used in the present experiment, the generated states have a much richer structure as is shown below.

Our experimental setup is presented in Fig. 2. Nearly Fourier-limited femtosecond pulses (180 fs, 40 nJ), produced by a Ti:sapphire laser with a 800 kHz repetition rate, are frequency doubled by a single pass in a 100 μm -thick type I noncritically phase-matched potassium niobate (KNbO₃) crystal. The frequency-doubled beam pumps an identical crystal used as an optical parametric amplifier (OPA), generating Gaussian quadrature-entangled pulses spatially separated by an angle of 10°. Adjusting the pump power allows us to vary the two-mode squeezing between 0 and 3.5 dB. The photon pickoff beam splitters are realized with a single polarizing beam splitter (PBS) cube, where the signal and idler beams are recombined spatially but remain separated in polarization. A small adjustable fraction R of both beams is sent into the APD channel, where they interfere on a

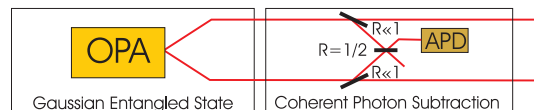


FIG. 1: Coherent photon subtraction from Gaussian entangled beams.

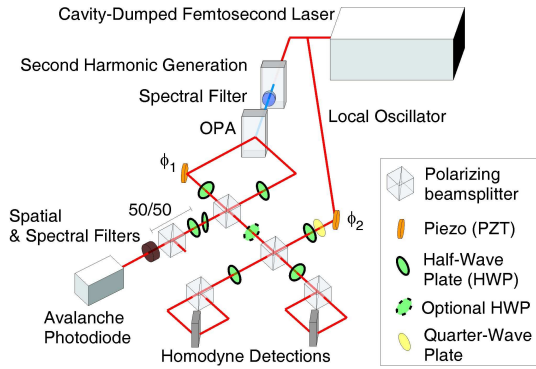


FIG. 2: Experimental setup.

50/50 BS. A tilted half-wave plate compensates for residual birefringence. An APD detects one of the 50/50 BS outputs after spatial and spectral filtering. The signal and idler beams transmitted through the pickoff beam splitter are projected into a non-Gaussian state by an APD detection. They are spatially separated on another PBS, where they are combined with bright local oscillator beams. A quarter-wave and a half-wave plate allow us to prepare two local oscillators with equal intensities and a well-defined relative phase. The signal and idler beams are analyzed by two time-resolved homodyne detections, which sample each individual pulse, measuring one quadrature $x_{1,2}(\theta_{1,2})$ in phase with the local oscillator.

In this setup, all the relative phases except ϕ_1 and ϕ_2 (see Fig. 2) are precisely adjusted with wave plates. Phase fluctuations concern only the initial two-mode squeezed state, where the phase difference is not defined and plays no role, and the slow (thermal and acoustic) phase sum fluctuations simply rotate the two-mode squeezing ellipse and can be compensated by shifting the common phase ϕ_2 of the local oscillators. This phase can be scanned with a piezo translator, and rapidly measured using the unconditioned two-mode squeezing variance.

Quantum states with negative Wigner functions are very sensitive to experimental imperfections. In our case, the most important issue are spurious APD trigger events, due to imperfect filtering, limited qualities of the optical beams, imperfect mode-matching between the subtracted beams, and APD dark counts. An APD count corresponds to the desired subtraction event with a success probability $\xi < 1$. This explains why single-photon protocols are more robust than two-photon ones, where the total success probability is only ξ^2 . Another issue is the OPA excess noise. To describe it, we can consider that a first amplification process creates a pure entangled state with a two-mode squeezing variance $s = e^{-2r}$, and that each of the resulting modes is independently amplified with a gain $h = \cosh^2(\gamma r)$ by a phase-independent amplifier with a relative efficiency γ . The finite homodyne efficiency η and the homodyne excess noise e also

deteriorate the measured data. However, they are not involved in the generation process but only in the analysis, and we can correct for their effects in order to determine the actual Wigner function of the generated state. Even with none of these imperfections, this protocol would still be limited by the finite pick-off BS reflectivity R , required for a sufficient APD count rate but inducing losses on the transmitted beam. The limited overall efficiency $\mu = 5\%$ of the APD channel has little effect in this experiment.

A detailed analytic model [16, 19] including all these imperfections yields an expression for the Wigner function W of the state studied in our experiment :

$$W(x_1, p_1, x_2, p_2) = W_s(x_+, p_+)W_c(x_-, p_-) \quad (1)$$

where $x_{\pm} = \frac{x_1 \pm x_2}{\sqrt{2}}$, $p_{\pm} = \frac{p_1 \pm p_2}{\sqrt{2}}$, W_s is the Wigner function of a single-mode squeezed state, and W_c corresponds to a photon-subtracted squeezed state analyzed in [19]. More explicitly :

$$\begin{aligned} W_s(x, p) &= \exp(-x^2/a - p^2/b) / (\pi\sqrt{ab}) \\ W_c(x, p) &= W_s(x, p) \left[\frac{2A}{a^2}x^2 + \frac{2B}{b^2}p^2 + 1 - \frac{A}{a} - \frac{B}{b} \right] \\ a(s) &= b(1/s) = 1 + e + \eta(1-R)(hs + h - 2) \\ A(s) &= B(1/s) = \frac{\eta \xi (1-R)(hs + h - 2)^2}{h(s + 1/s) + 2h - 4} \end{aligned}$$

In this experiment the photon-subtracted state is “delocalized” into two spatially separated modes 1 and 2 and revealed by measuring the correlations between identical quadratures, the anticorrelations remaining in the initial squeezed state.

Without assuming any particular shape for W_s and W_c , we can experimentally show that the state becomes separable if we make a joint measurement, transforming $x_{1,2}$ into x_{\pm} by rotating the polarizations by 45° with the optional half-wave plate shown on Fig. 2. We then observe that the quadratures measured by one detection do not depend on the other (see Fig. 3). For every θ_{\pm} the joint distribution, and hence the Wigner function, becomes factorable : $P(x_+(\theta_+), x_-(\theta_-)) = P_s(x_+(\theta_+))P_c(x_-(\theta_-))$. It means that one can fix $\theta_- = \theta_+ = \theta$ and scan θ to perform a complete tomography of this state.

This property considerably simplifies the experimental analysis. We perform direct homodyne measurements of the entangled quadratures $x_{1,2}(\theta)$, keeping the entangled modes 1 and 2 separated without mixing them. We use the fact that the state factorizes in the x_+, x_- basis to reconstruct it from a limited set of data : instead of a time-consuming general two-mode tomography, which requires to measure $x_1(\theta_1), x_2(\theta_2)$ with all possible combinations of phases, we can restrict ourselves to $\theta_1 = \theta_2 = \theta$. In practice, we set the relative phase between the local oscillators to zero, scan the common phase $\phi_2 = \theta$, measure $x_{1,2}(\theta)$ and calculate $x_{+,-}(\theta)$. We reconstruct the distributions $P_c(x_-(\theta))$ and $P_s(x_+(\theta))$ for several phases. We

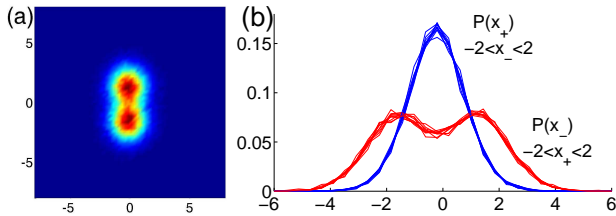


FIG. 3: State separability test after interference between signal and idler beams : (a) Joint distribution $P(x_+, x_-)$, (b) Distributions $P_s(x_+)$ and $P_c(x_-)$, for 11 values of x_- (resp. x_+), chosen between -2 and +2. This separability was verified for several randomly chosen values of θ_+ and θ_- (here $\theta_+ = 20^\circ$ and $\theta_- = 50^\circ$).

observe that the measured distributions are invariant under $\theta \rightarrow \pi \pm \theta$, so we restrict the analysis to $0 \leq \theta \leq \pi/2$. Typically, we measure 6 to 12 different quadrature distributions, with 10000 to 20000 data points each. A numeric Radon transform allows us to reconstruct the uncorrected Wigner functions W_c and W_s . We can correct for the homodyne detection losses ($\eta = 70\%$, $e = 1\%$ of the shot noise) using a maximal-likelihood algorithm [25, 26] to obtain the Wigner function W of the generated state. We use W to calculate the density matrix ρ of the state and obtain its entanglement, given by the negativity $\mathcal{N} = \frac{\|\rho^{T_1}\|_1 - 1}{2}$, where T_1 is the partial transposition operation [22].

Figure 4 presents the tomography of a state produced with 1.8 dB of squeezing and a BS reflectivity $R = 5\%$. The Wigner function, corrected for detection losses, is clearly negative : $W_c(0) = -0.13 \pm 0.01$ (0.01 ± 0.01 before correction). The entanglement of this state is $\mathcal{N} = 0.34 \pm 0.02$, whereas for the initial state (before the pickoff BS) $\mathcal{N}_0 = 0.24 \pm 0.01$.

In Refs. [16, 19] we demonstrated another analysis method, more constrained but also much faster and closer to the physics of the experiment. If we assume that the Wigner function has the form defined in Eq. 1, we can easily extract the parameters a , A , b , B from the second and fourth moments of the measured distributions, and determine the Wigner function, the density matrix, and the quadrature distributions of the measured state. For a given squeezing, one can also obtain from a , A , b and B the values of all the experimental parameters introduced above. To correct for homodyne losses, we simply calculate the Wigner function that we would measure with an ideal detection ($\eta = 1$ and $e = 0$), using the values extracted from the experimental data for all the other parameters. As shown in Fig. 4, the distributions reconstructed with this method are in excellent agreement with those directly extracted from the data, and the Wigner function is almost indistinguishable from the one obtained with the maximal-likelihood algorithm. Both methods give the same values for the negativity.

A natural question to ask is whether this protocol

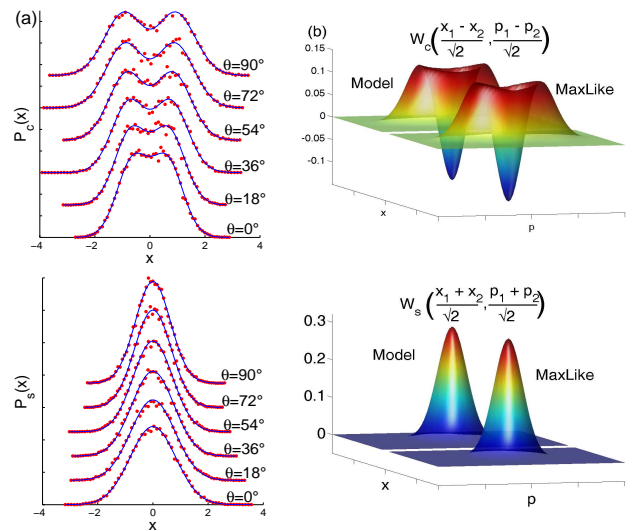


FIG. 4: (a) Set of experimentally measured quadrature distributions (dots), compared to those reconstructed from our model (solid line). (b) Wigner function corrected for homodyne detection losses, obtained with a standard maximal-likelihood algorithm (MaxLike), compared to the result of our model. This state is produced with 1.8 dB of squeezing and $R = 5\%$.

works for an arbitrary squeezing or if, when the initial state is already strongly entangled, by performing an imperfect photon subtraction we actually lose more entanglement than we gain. It has already been shown that, when the pick-off beam splitters have a finite reflectivity, subtracting one photon from each of the Gaussian entangled beams may actually decrease the entanglement [10]. Using our model, we can take into account all the other experimental parameters to derive an analytic expression for ρ^{T_1} , which can be diagonalized numerically in a few seconds to obtain the expected negativity of a given state. We found that the experimental imperfections have a very strong effect. For example, for an initial squeezing of 3 dB, the negativity increases ideally from $\mathcal{N}_0 = 0.50$ to $\mathcal{N} = 0.90$. If we assume $R = 3\%$ for the

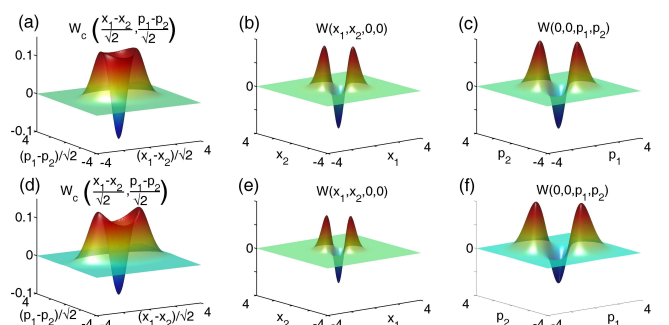


FIG. 5: Tomography of two states produced with 1.3 dB (first row) and 3.2 dB (second row) of squeezing and $R = 10\%$: three different cuts of the two-mode Wigner function.

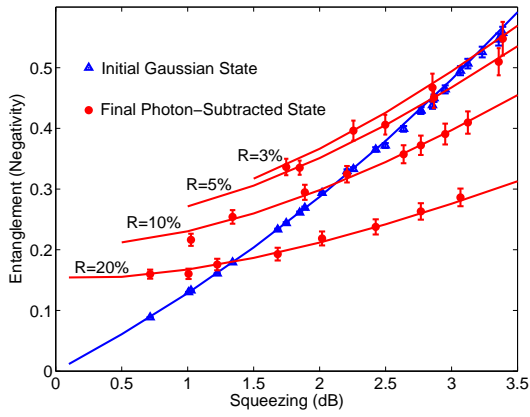


FIG. 6: Entanglement negativity of the initial and final states as a function of squeezing for several pickoff BS reflectivities, corrected for homodyne detection losses. Solid lines are theoretical calculations using the average values of the experimental parameters.

pick-off BS, then $\mathcal{N} = 0.81$, but if we include the average values of experimental parameters involved in the state preparation, $\langle \gamma \rangle = 0.22$ and $\langle \xi \rangle = 0.78$, \mathcal{N} drops down to 0.51, whereas for the initial state, only slightly affected by γ , $\mathcal{N}_0 = 0.49$.

To verify this experimentally, we performed several tomographies for different BS reflectivities and degrees of squeezing. Figure 5 presents two tomographies with $R = 10\%$ for a small (1.3 dB) and a high (3.2 dB) squeezing. As expected, the Wigner function becomes more phase-dependent and less negative as the state becomes “bigger” and more sensitive to decoherence.

Figure 6 shows the entanglement negativity of the photon-subtracted states and the corresponding initial states. The solid lines are theoretical calculations using the average values of the experimental parameters involved in the state preparation, $\langle \gamma \rangle = 0.22$ and $\langle \xi \rangle = 0.78$. Two domains appear on the graph: the upper left, where this process actually increases the entanglement, and the lower right, where the initial state is too sensitive to the added losses. As expected, this protocol is particularly efficient at low squeezing. One can show that when the squeezing and hence the entanglement of the initial state tend to 0, the negativity of the final state has a nonzero limit $\mathcal{N}_{r \rightarrow 0} = \frac{\sqrt{C^2 + (1-C)^2} - (1-C)}{2}$ where $C = \frac{\xi(1-R)}{1+\gamma^2}$. At low squeezing, experimental imperfections have a moderate effect on the state. We nevertheless succeed in improving the negativity of a state with up to 3 dB of squeezing, which corresponds to a strong squeezing regime where small experimental improvements strongly affect the performance of the protocol. For example, increasing ξ by a mere 4% with $R = 3\%$ should displace the crossover point from 3 to 4 dB (in other experiments, where mode matching between subtracted photons was not an issue, ξ reached 0.9

[16]).

In conclusion, the present photon subtraction protocol allows one to increase the entanglement between Gaussian states with up to 3 dB of squeezing, and even small experimental improvements should significantly increase this limit. For QIP protocols specifically requiring Gaussian entanglement, these non-Gaussian states could in principle be used as a starting point for a “Gaussification” procedure [9]. This demonstrates one of the key steps required for long distance quantum communications with continuous variables.

This work is supported by the EU IST/FET project COVAQIAL, and by the French ANR/PNANO project IRCOQ.

* Electronic address : alexei.ourjountsev@institutoptique.fr

- [1] C. H. Bennett *et al.*, Phys. Rev. A **53**, 2046 (1996).
- [2] Paul G. Kwiat *et al.*, Nature **409**, 1014 (2001).
- [3] Jian-Wei Pan *et al.*, Nature **423**, 417 (2003).
- [4] P. Walther *et al.*, Phys. Rev. Lett. **94**, 040504 (2005).
- [5] J. Eisert, S. Scheel, and M. B. Plenio, Phys. Rev. Lett. **89**, 137903 (2002).
- [6] J. Fiurášek, Phys. Rev. Lett. **89**, 137904 (2002).
- [7] G. Giedke and J. I. Cirac, Phys. Rev. A **66**, 032316 (2002).
- [8] Lu-Ming Duan *et al.*, Phys. Rev. Lett. **84**, 4002 (2000).
- [9] J. Eisert and *et al.*, Annals of Physics **311**, 431 (2004).
- [10] Akira Kitagawa *et al.*, Phys. Rev. A **73**, 042310 (2006).
- [11] T. Opatrný, G. Kurizki, and D.-G. Welsch, Phys. Rev. A **61**, 032302 (2000).
- [12] P. T. Cochrane, T. C. Ralph, and G. J. Milburn, Phys. Rev. A **65**, 062306 (2002).
- [13] S. Olivares, M. G. A. Paris, and R. Bonifacio, Phys. Rev. A **67**, 032314 (2003).
- [14] A. I. Lvovsky *et al.*, Phys. Rev. Lett. **87**, 050402 (2001).
- [15] A. Zavatta, S. Viciani, and M. Bellini, Phys. Rev. A **70**, 053821 (2004).
- [16] A. Ourjountsev, R. Tualle-Brouiri, and P. Grangier, Phys. Rev. Lett. **96**, 213601 (2006).
- [17] S. A. Babichev, J. Appel, and A. I. Lvovsky, Phys. Rev. Lett. **92**, 193601 (2004).
- [18] Milena D’Angelo *et al.*, arXiv:quant-ph/0602150 (2006).
- [19] A. Ourjountsev *et al.*, Science **312**, 83 (2006).
- [20] J. S. Neergaard-Nielsen *et al.*, Phys. Rev. Lett. **97**, 083604 (2006).
- [21] J. Wenger *et al.*, Eur. Phys. J. D **32**, 391 (2005).
- [22] G. Vidal and R. F. Werner, Phys. Rev. A **65**, 032314 (2002).
- [23] R. García-Patrón *et al.*, Phys. Rev. Lett. **93**, 130409 (2004).
- [24] H. Nha and H. J. Carmichael, Phys. Rev. Lett. **93**, 020401 (2004).
- [25] J. Řeháček, Z. Hradil, and M. Ježek, Phys. Rev. A **63**, 040303(R) (2001).
- [26] A. I. Lvovsky, J. Opt. B: Quantum Semiclass. Opt **6**, S556 (2004).